



Chitosan beads as barriers to the transport of azo dye in soil column

Nikolaos K. Lazaridis^{a,*}, Helen Keenan^b

^a Division of Chemical Technology, School of Chemistry, Aristotle University of Thessaloniki, GR-541 24 Thessaloniki, Greece

^b Department of Civil Engineering, 107 Rottenrow, University of Strathclyde, Glasgow G4 0NG, United Kingdom

ARTICLE INFO

Article history:

Received 26 March 2009

Received in revised form 22 July 2009

Accepted 14 August 2009

Available online 22 August 2009

Keywords:

Chitosan
Reactive barriers
Sorption
Dye

ABSTRACT

The development of chitosan-based materials as useful adsorbent polymeric matrices is an expanding field in the area of adsorption science. Although chitosan has been successfully used for the removal of dyes from aqueous solutions, no consideration is given to the removal of dyes from contaminated soils. Therefore this study focuses on the potential use of chitosan as an *in situ* remediation technology. The chitosan beads were used as barriers to the transport of a reactive dye (Reactive Black 5, RB5) in soil column experiments. Batch sorption experiments, kinetic and equilibrium, were performed to estimate the sorption behavior of both chitosan and soil. The chitosan beads were prepared in accordance with published literature and a synthetic soil was prepared by mixing quantities of sand, silt and clay. The synthetic soil was classified according to British Standards. Calcium chloride was used as tracer to define transport rates and other physical experimental parameters. Dye transport reaction parameters were determined by fitting dye breakthrough curves (BTCs) to the HYDRUS-1D version 4.xx software. Fourier Transform-Infrared (FT-IR) spectroscopy was used to reveal the sorption mechanism. The study showed that chitosan exhibited a high sorption capacity ($S_{\max} = 238 \text{ mg/g}$) and pseudo-first sorption rate ($k_1 = 1.02 \text{ h}^{-1}$) coupled with low swelling and increased retardation for the azo dye tested. Thus it has potential as a Permeable Reactive Barrier (PRB) for containment and remediation of contaminated sites.

© 2009 Elsevier B.V. All rights reserved.

1. Introduction

Azo dyes represent the largest class of dyes applied in textile processing. The degree of fixation of dyes to fabrics is never complete, resulting in dye-bearing effluents. The removal of dyes from these effluents is desired, not only for aesthetic reasons, but also because many azo dyes and their breakdown products are toxic to aquatic life and mutagenic to humans [1,2].

Several methods have been developed to remove color from dye-house effluent, varying in effectiveness, economic cost and environmental impact. Traditionally, biological treatments using activated sludge have been used. They can reduce Biological Oxygen Demand, but do not effectively remove color, as the oxidation rate is very slow [3]. Sorption of dye molecules onto a biosorbent can be a very effective, alternative to activated carbon, low cost method of color removal [4].

Numerous studies have investigated either the sorption of dyes to various low cost sorbents as a wastewater treatment method [5,6] or the use of dyes as tracers for soil hydrology [7]. However, there is no special mention about the fate of unsuccessfully treated dyes in soils and potential *in situ* clean-up technology.

To date, mostly conventional remediation technologies (e.g., pump-and-treat systems) have been applied for the clean up of contaminated groundwater. Even after many years of operation, however, it has proven difficult and costly to meet clean-up standards. Lately, there has been an explosion of activity directed at the development and implementation of Permeable Reactive Barriers (PRBs) also known as treatment walls [8,9]. PRBs involve construction of permanent, semi-permanent or replaceable units across the path of a dissolved phase contaminant plume [10]. PRBs constitute a semi passive, *in situ* remediation technology that utilizes reactive media which cause physical/chemical or biochemical reactions to transform or immobilize contaminants.

The media for physical reactions are evaluated based on: (i) high sorption capacity; (ii) sufficiently rapid rates; (iii) negligible desorption and (iv) the ability to maintain adequate permeability and reactivity over a long time period. Iron metal is the most frequently utilized medium, accounting for approximately 45% of PRBs. However, a significant drawback is the oxidation of iron and precipitation of oxides that may clog the pore space [8].

The purpose of this study was to assess chitosan beads as potential barriers to the transport of azo dye in soil column. Chitosan is derived from chitin one of the most abundant natural biopolymers. Chitin itself is mostly found in the exoskeletons of crustaceans, molluscs and in the cell walls of micro-organisms; however chitosan produced by the de-acetylation of chitin produces a more adsorbent material [11]. It is known that chitosan is an effective sorbent

* Corresponding author. Tel.: +30 32310 997807; fax: +30 32310 997859.
E-mail address: nlazarid@chem.auth.gr (N.K. Lazaridis).

Table 1
Particle size analysis of artificial soil and chitosan beads.

Material	$D_{0.1}$ (μm)	$D_{0.5}$ (μm)	$D_{0.9}$ (μm)
Soil	91	787	1366
Chitosan	64	452	868

for most dye classes [12]. The chitosan beads used in this study, with a low swelling percentage, were prepared by a novel cross-linking procedure and were found effective for the sorption of dyes in previous batch experiments [13].

2. Experimental

2.1. Materials

High-molecular weight chitosan (Ch) was obtained from Sigma–Aldrich and purified by extraction with acetone in a Soxhlet apparatus for 24 h, followed by drying under vacuum at room temperature. The average molecular weight was estimated to be 3.55×10^5 and the degree of de-acetylation was 82 wt%. Glutaraldehyde (GA, 50 wt% in water, Sigma–Aldrich) was used in the preparation of the beads. The tracer calcium chloride-2 hydrate was purchased from BDH. The reactive azo dye Reactive Black 5 ($\text{C}_{26}\text{H}_{25}\text{O}_{19}\text{N}_5\text{S}_5$) was kindly supplied by Dye Star. The maximum absorption wavelength for the dye solutions was determined by running full-range wavelength scans. Fig. 1 presents the chemical structure of Reactive Black 5.

Chitosan beads were prepared according to previously published work [13]. Briefly, 0.5 g chitosan was dissolved in 50 mL of an aqueous 2% (v/v) CH_3COOH solution. The solution was added drop wise from a pipette into an aqueous solution of GA 5.01 g/L, which also contained 5.00 g tripoly phosphate (TPP) at pH 6, adjusted with an aqueous HCl solution. The formed gelled microspheres were stirred overnight at room temperature in the aforementioned solution. Then, they were filtered and purified by extraction with water in a Soxhlet apparatus for 24 h. The drying of beads was carried out at 323 ± 1 K.

The synthetic soil material was prepared by mixing sand, silt and clay. The sand was commercial British sand. Silt was taken from a bank of the river Clyde, 15 km from Glasgow. The clay, classified as stiff clay, was excavated from the Hallyard Quarry 30 km from Glasgow. The mixing of the three constituents was done in the ratio, sand:silt:clay (85:10:5).

A particle size micro-analyzer (Malvern Master Sizer 2000) was used to determine the particle size distribution of the simulated soil and chitosan, by laser light scattering. Average particle size was expressed as the volume mean diameter ($D_{4.3}$). $D_{0.9}$, $D_{0.5}$ and $D_{0.1}$ are the particle diameters determined respectively at the 90th, 50th and 10th percentile of undersized particles. The results are given in Table 1. The simulated soil could be classified as loamy sand soil according to British Standards [14].

FT-IR spectra of pure soil components and chitosan along with the respective dye-loaded materials were obtained by a PerkinElmer FT-IR spectrophotometer, model Spectrum 1000, in the range of $4000\text{--}500\text{ cm}^{-1}$ using KBr pellets containing the prepared materials. The resolution for each spectrum was 2 cm^{-1} and

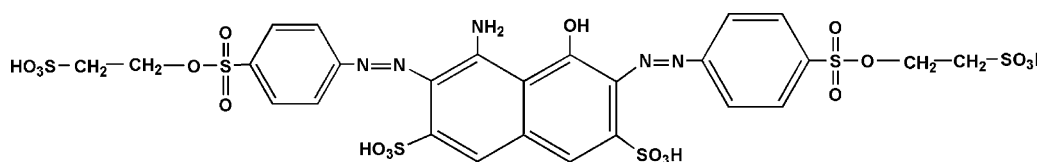


Fig. 1. Chemical structure of the dye Reactive Black 5.

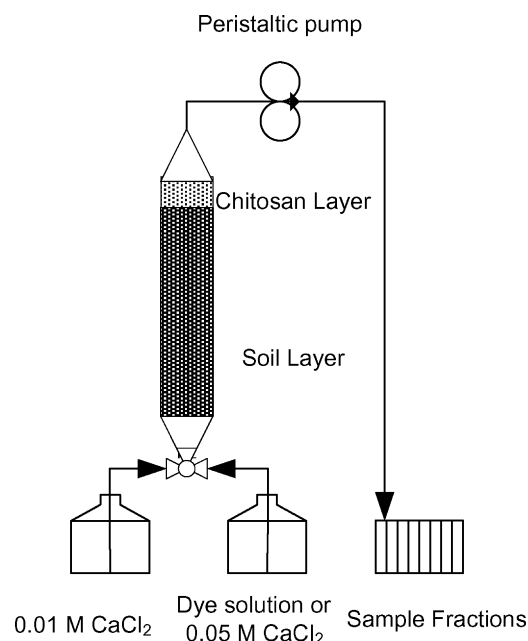


Fig. 2. Experimental set-up.

the number of co-added scans was 64. The spectra presented are baseline corrected and converted to the absorbance mode.

2.2. Batch equilibrium/kinetic experiments

For equilibrium experiments, a constant amount of soil or chitosan was mixed with 25 mL of various initial dye solutions ($\text{pH}_{\text{in}} 6.5$) into glass vials [15]. For kinetic experiments, 2.5 g soil or 0.025 g chitosan were mixed with 25 mL of 20 mg/L or 100 mg/L dye solutions into glass vials. The background electrolyte was 0.01 mol/L CaCl_2 , according to the OECD Test Guideline 106 [16], and the final $\text{pH} 5.50 \pm 0.50$. The CaCl_2 solution is used as the aqueous solvent phase to improve centrifugation and minimize cation exchange of the soil. The slurries were agitated by rotation of the vials top to bottom (1.5 rps) at constant temperature (293 ± 1 K) for pre-determined time intervals. After completion of agitation (24 h for equilibrium experiments), the vials were centrifuged at 1700 rpm and aliquots were removed and analyzed. Each experiment was replicated 3 times.

2.3. Column dynamic experiments

A Teflon (polytetrafluoroethylene, PTFE) column (Fig. 2) with a diameter of 2.6 cm was packed with 110 g dry soil to a length of approximately 12 cm. The column was saturated from the bottom up, over 24 h, using a solution of 0.01 mol/L CaCl_2 . After the column was saturated, and steady state flow was achieved, three breakthrough curves (BC) were run at a flow rate of $42\text{ cm}^3/\text{h}$ [17]: (i) Tracer–Soil BC: a solution pulse of 0.05 mol/L CaCl_2 was introduced to characterize the transport (hydrodynamics) through the column. Following completion of the non-reactive pulse, the col-

umn was flushed with 0.01 mol/L CaCl₂ to elute the tracer from the column; (ii) Dye–Soil BC: a solution pulse of 30 mg/L dye was introduced to determine retention behavior of dye by the soil column. Following completion of the dye pulse, the column was flushed with 0.01 mol/L CaCl₂ to elute the dye from the column and (iii) Dye–Soil/Chitosan BC: in this case, chitosan beads (4 g) were placed at the top of the column. After the column was saturated, and steady state flow was achieved, a solution pulse of 30 mg/L dye was introduced to determine retention behavior of dye by the soil/chitosan column. In all cases, effluent samples were collected periodically and analyzed.

2.4. Analysis

Reactive (dye) and non-reactive (chloride) samples of the solutions were collected at various time intervals and analyzed using a UV–Vis spectrophotometer (UV/Vis 6405, Jenway) and a conductivity meter (PCM3, Jenway), respectively. The effect of pH over the calibration curve of dye was studied prior to the sorption experiments, as the λ_{\max} of the dye solution may be pH dependent, but no significant deviation was observed. The amount of dye sorbed, S (M/M), was calculated using the mass balance equation:

$$S = \frac{(C_0 - C)V}{m} \quad (1)$$

where C_0 (M/L³) is the initial solute concentration, V (L³) is the volume and m (M) mass of the sorbent.

3. Results and discussion

3.1. Batch equilibrium experiments

The movement of a sorbing solute is retarded relative to the mean water flow because of partitioning of the solute between the liquid and the solid phase, so that

$$C^T = \theta C + \rho_b S \quad (2)$$

where C^T (M/L³) is the total solute concentration, θ the effective volumetric content of the soil (L³/L³), ρ_b (M/L³) is the bulk density.

Assuming equilibrium interaction between the solution concentration C_e (M/L³) and sorbed concentration S^e (M/M), then the sorption isotherm is described by a generalized non-linear Langmuir–Freundlich equation of the form [18]:

$$S^e = \frac{S_{\max} \eta C_e^\beta}{1 + \eta C_e^\beta} \quad (3)$$

where S_{\max} (M/M) is the maximum sorption concentration; η (L³/M)^{1/β} is a constant and β (–) is the heterogeneity constant.

Equilibrium experiments are a prerequisite to understand the dye–solid interaction. Equilibrium data for soil and chitosan are given in Fig. 3. There is an initial steep ascent which is followed by a slower approach until a plateau is reached. The data were successfully correlated ($R^2 > 0.995$) with the non-linear Langmuir–Freundlich equation. It is easily observable the low affinity of the reactive dye for the soil ($S_{\max} = 0.017$ mg/g) and the strong one for the polymeric matrix ($S_{\max} = 238$ mg/g). Table 2 presents the adsorption capacities of various sorbents for Reactive Black 5. Chitosan beads exhibit a significant high capacity, but not the highest. However, a direct comparison among materials could be misleading because of the different applied experimental conditions. In this study, experiments have been performed (i) at pH 5.50 ± 0.50, which is not optimum (pH_{opt} 2.0) and (ii) in the presence of background electrolyte (0.01 mol/L CaCl₂), which also reduces the sorption loading [32]. On the other hand, high sorption capacity

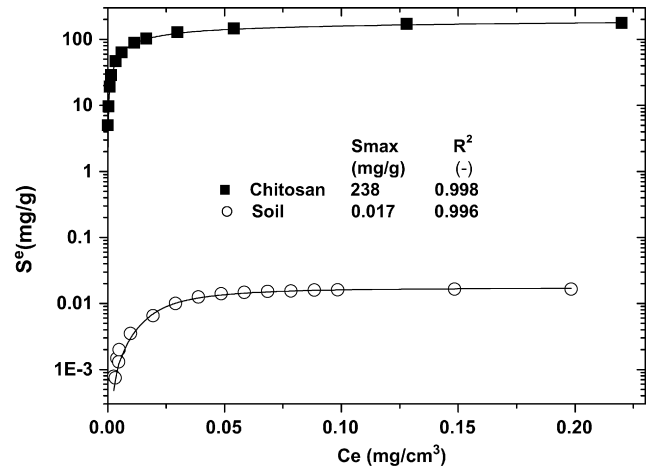


Fig. 3. Equilibrium data for the systems soil–reactive dye and chitosan–reactive dye. Solid lines present Langmuir–Freundlich equation.

Table 2

Comparison of adsorption capacities of various sorbents for Reactive Black 5.

Adsorbent	S_{\max} (mg/g)	Reference
Chitosan	1000	[19]
Chitosan	936	[20]
Mesoporous activated carbon	600	[21]
<i>Corynebacterium glutamicum</i>	419	[22]
Chitosan beads	238	This study
Modified polymeric sorbent	159	[23]
Surfactant modified activated carbon	129	[24]
Dried activated sludge	116	[25]
Furnace slag	109	[26]
<i>Aspergillus foetidus</i>	106	[27]
Powder activated carbon	59	[28]
Barley straw	25	[29]
Fly ash	8	[30]
Biomass fly ash	4	[28]
Sunflower seed shells	1	[31]

does not guarantee the proper mechanical and swelling behavior of sorbents as reactive barriers.

3.2. Batch kinetic experiments

Fig. 4 depicts the effect of contact time on the sorption behavior of the simulated soil and chitosan beads. For materials, the

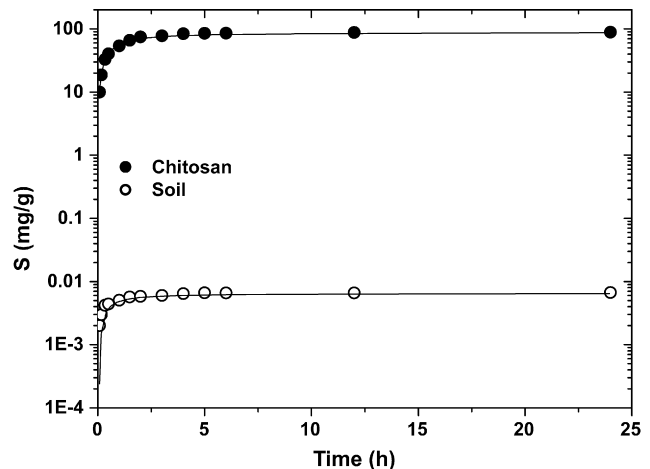


Fig. 4. Batch kinetic data for the systems soil–reactive dye and chitosan–reactive dye. Solid lines present the modified second-order kinetic model.

Table 3
Parameters of the three kinetic models for the adsorption of RB5 onto chitosan and soil.

Material	Pseudo-first order		Pseudo-second order		Modified second order	
	k_1 (h ⁻¹)	R^2	k_2 (h ⁻¹)	R^2	k_m (h ⁻¹)	R^2
Chitosan	1.02	0.984	1.88	0.989	1.94	0.990
Soil	1.38	0.956	2.51	0.959	3.17	0.979

high sorption rates at the beginning of adsorption followed by a flat plateau (saturation values) and equilibrium were reached at approximately 5 h. The collected data sets were fitted to the pseudo-first order model (Eq. (4)), the pseudo-second order model (Eq. (5)) and the modified second order model (Eq. (6)) [33,34]

$$S = S^e(1 - e^{-k_1 t}) \tag{4}$$

$$S = S^e \left(1 - \frac{1}{1 + k_2 t} \right) \tag{5}$$

$$S = S^e \left(1 - \frac{1}{\beta_2 + k_m t} \right) \tag{6}$$

where β_2 is a parameter of the modified second order model and k_1 , k_2 , k_m are the sorption rate coefficients (h⁻¹) for the pseudo-first, the pseudo-second and the modified second order model, respectively. The resulting kinetic parameters are given in Table 3, while the respective S^e values have been determined experimentally. The adsorption rates show that chitosan and soil present approximately the same sorption rate but with a vastly difference in the sorption loading. A high correlation obtained between the experimental data and all kinetic models. Precisely, the highest correlation was achieved by the modified second order because of the extra degree of freedom (β_2), which makes the model more flexible.

Equilibrium and kinetic data analysis was performed using non-linear least-square fitting. A Levenberg–Marquardt algorithm was used to iteratively search for the parameters that best fit the data, determined by minimization of the χ^2 value [35].

3.3. Column dynamic experiments

The tracer and dye displacement experiments were inversely modeled using the program HYDRUS-1D version 4.xx [36]. This inverse model routine uses a least-squares method that minimizes an objective function, which provides a best-fit model solution to the measured transport data. The best-fit model solution to the transport data is obtained by finding the optimum combination of reaction and transport parameters [37].

Fig. 5a illustrates the measured and fitted breakthrough curves for the tracer in the soil column. The recorded data were almost symmetrical indicating an ideal transport behavior. Soil hydraulic characteristics were estimated by employing pedotransfer functions (PTFs) that use widely available basic soil data (texture, bulk density, etc.) as predictors. Rosetta, a build in HYDRUS file, implements PTFs to predict water retention parameters and saturated hydraulic conductivity (K_s) by using textural class, textural distribution, bulk density. The estimated parameters were used for the rest of experiments.

Fig. 5b and c depicts the measured and fitted breakthrough curves for the dye in the absence and presence of reactive barrier. Various sorption concepts are available to describe the interaction of dissolved substances with the solid material. These sorption concepts differ with respect to the involved sorption isotherm (linear or non-linear), the assumptions made concerning the time-dependency (instantaneous or rate-limited) and reversibility of the sorption process (reversible or irreversible) [38].

The non-equilibrium transport models are divided into three groups: (i) physical, (ii) chemical and (iii) physical and chemical non-equilibrium transport. After testing, the chemical non-

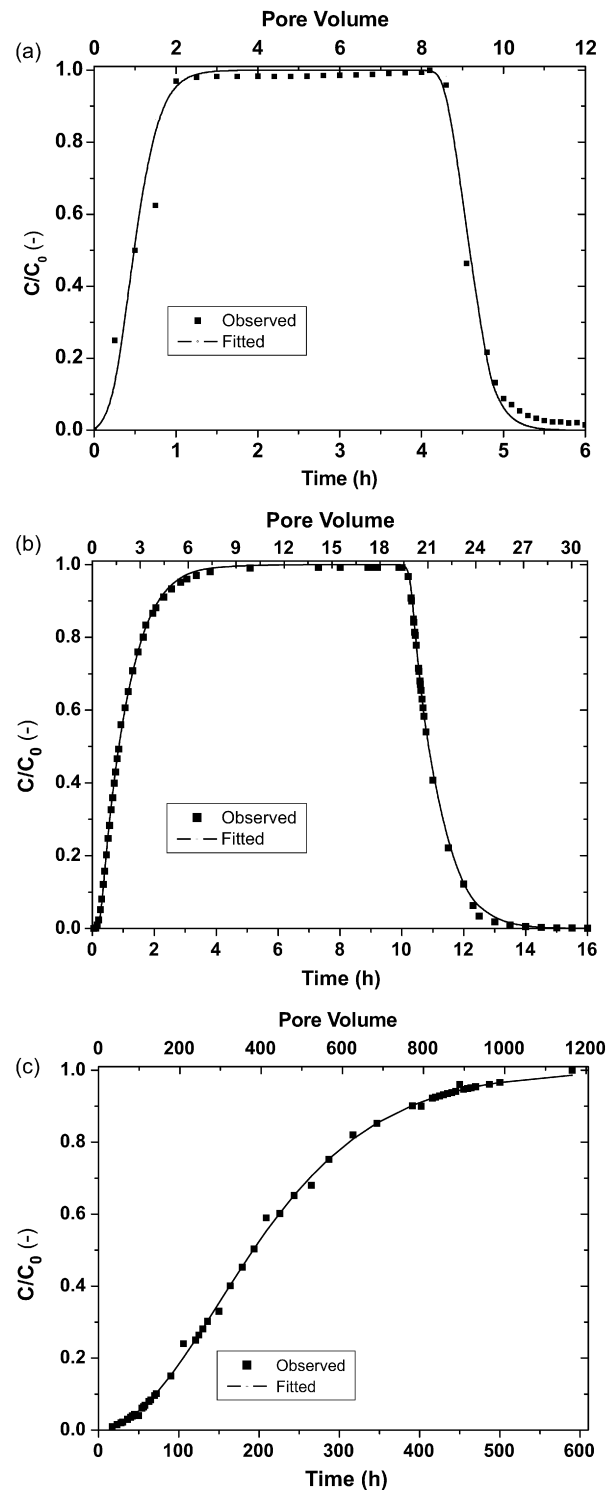


Fig. 5. Measured and predicted breakthrough curves for: (a) Cl⁻ in soil column; (b) dye in soil column; (c) dye in soil column equipped with a chitosan treatment wall.

equilibrium employing the attachment–detachment approach was used to describe effectively the transport data. In this case, the relatively standard advection–dispersion transport equation (ADE–Eq. (7a)) is supplemented with Eq. (7b) describing the attachment–detachment of a solute:

$$\theta \frac{\partial C}{\partial t} + \rho_b \frac{\partial S^k}{\partial t} = \theta D \frac{\partial^2 C}{\partial x^2} - q \frac{\partial C}{\partial z} \quad (7a)$$

$$\rho_b \frac{\partial S^k}{\partial t} = \theta k_{a1} C - \rho_b k_{d1} S^k \quad (7b)$$

where S^k (M/M) is the sorbed concentration of the kinetic sorption sites, q (L/T) is the volumetric water flux density, D (L²/T) is the global dispersion coefficient accounting for both molecular diffusion and hydrodynamic dispersion and k_{a1}/k_{d1} are the attachment/detachment rate coefficients (h⁻¹). The global dispersion coefficient is given by the relationship $D = \lambda v + D_0$, where λ is the dispersivity (L) and D_0 the molecular diffusion coefficient. The solute transport equations were solved using the Galerkin finite element method with a Crank–Nicholson time weighting scheme.

The mean travel times of the conservative (μ^c) or partitioning (μ^p) solutes were determined from moment analysis of the breakthrough curves [39]:

$$\mu = \frac{\int_0^{t_F} t C dt}{\int_0^{t_F} C dt} - \frac{t_p}{2} \quad (8)$$

where t_F is the time the solute measurements were terminated and t_p is the duration of pulse input. The retardation factor, R , was calculated from the following equation

$$R = \frac{\mu^p}{\mu^c} \quad (9)$$

The resulted transport parameters for the dynamic experiments are given in Table 4. One may discern the impact of chitosan reactive barrier in the breakthrough curves of soil column. Chitosan resulted in a significant increase in the retardation factor (~80 times), an increase in the attachment rate (~7 times) and decrease in the detachment rate (~56 times). The latter is consistent with batch desorption experiments of loaded chitosan which showed an almost irreversible sorption behavior.

The amount of dye retained by chitosan ($m_{ret} = 269.4$ mg) was determined by subtracting the eluted mass ($m_{out} = 473.8$ mg), which was determined by integrating under the breakthrough curve, from the total injected mass of dye ($m_{tot} = 743.4$ mg). Therefore, the resulting sorption capacity of chitosan beads is 65.85 mg/g. The latter value shows a 3-fold decrease in the predicted adsorption maximum from batch experiments. This behavior is consistent with previously reported. In general, batch processes do not duplicate the hydrodynamic conditions of fixed-bed. Greater adsorption on batch compared to flow system is commonly reported in the literature [40]. The discrepancy implies mass transfer limitations due to shallow layer of chitosan which causes uneven flow patterns. However, a longer barrier layer bounded on down gradient side by a thin section of sand could improve flow and subsequently the adsorption capacity.

Table 4
Transport parameters for the dynamic experiments ($\rho_b = 1.74$ g/cm³, $\theta = 0.343$).

Solute	Sorbent	λ (cm)	k_{a1} (h ⁻¹)	k_{d1} (h ⁻¹)	R (–)	R^2
Tracer	Soil	1.2 ± 0.1	–	–	1.0	0.984
Dye	Soil	1.2 ± 0.1	3.0 ± 0.05	2.8 ± 0.06	2.1	0.996
Dye	Soil + Chitosan	1.2 ± 0.1	20.8 ± 0.6	0.050 ± 0.001	160	0.995

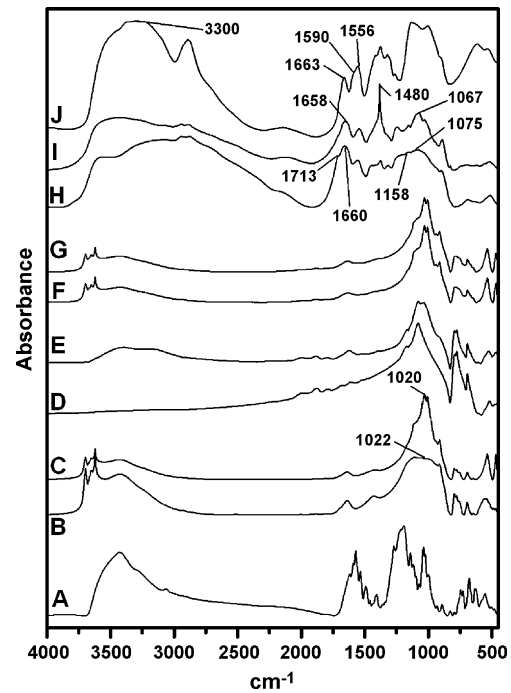


Fig. 6. FT-IR spectra of non-loaded and dye-loaded materials: (A) Reactive Black 5; (B) clay; (C) dye-loaded clay; (D) sand; (E) dye-loaded sand; (F) silt; (G) dye-loaded silt; (H) chitosan beads; (I) dye-loaded chitosan beads; (J) pure commercial chitosan.

3.4. Sorption mechanism

The comparison of the FT-IR spectra of the soil components and chitosan (dye-loaded and non-loaded) is given in Fig. 6. It is clear that the chitosan beads present shifts in their peaks before (non-loaded materials) and after sorption (loaded materials). Firstly, a comparison was realized between the FT-IR spectrum of the pure commercial chitosan (J) and the respective cross-linked chitosan beads (non-loaded material) (H). In particular, the amide I and II adsorption bands of chitosan are situated at 1663 and 1556 cm⁻¹ (J), respectively. The amide II band overlaps the asymmetric –NH₂ bending band at ~1590 cm⁻¹, the presence of which is confirmed by the adsorption at 1420 cm⁻¹, which is related to the presence of –NH₂ groups. The absorption bands at 1133 (asymmetric stretching of the C–O–C bridge), 1090 and 1005 cm⁻¹ (skeletal vibrations involving CO stretching) are characteristic of the polysaccharide structure of chitosan [41]. The broad band at ~3300 cm⁻¹ is attributed to the stretching vibration of O–H, extension vibration of N–H and inter-hydrogen bonds of the polysaccharide. The presence of the P=O groups in cross-linked chitosan beads is indicated by the peak at the frequency of 1158 cm⁻¹ (H). Furthermore, a broad shoulder that appears around ~2500 cm⁻¹ can be assigned to the –NH₂⁺ band [42]. The appearance of a strong peak at 1660 cm⁻¹ corresponds to the imine moiety formed as a result of the reaction between the free amino groups on the chitosan backbone and the aldehyde groups of the cross-linker (glutaraldehyde). The carbonyl group of the free unreacted end of some glutaraldehyde molecules results in the observed shoulder at 1713 cm⁻¹. The peak

of the ether group becomes stronger and is shifted to 1075 cm^{-1} , suggesting the formation of a new open chain ether linkage after the cross-linking [43]. Moreover, observing the spectrum of the loaded chitosan beads (I), the most characteristic peak of chitosan (carbonyl peak) presented a shift from 1660 (H) to 1658 cm^{-1} (I). Besides, the peak of the phosphate ions (originated from the tripolyphosphate sodium used as ionic cross-linker) was shifted from 1075 (H) to 1067 cm^{-1} (I). A presence of a strong peak at 1480 cm^{-1} (I) was observed, which is attributed to the interaction of dye molecule with the chitosan backbone. In this pH range, the interaction could be attributed to a combination of electrostatic interactions, van der Waals forces and hydrogen bonding [13].

On the contrary, the soil components clay, sand and silt did not present significant shifts of their FT-IR peaks. Only clay presented a significant shift of their peaks before and after sorption. The broad band at 1022 cm^{-1} of non-loaded clay (B) was replaced by a sharp and intense peak with higher absorbance at 1020 cm^{-1} (C). The other two components (sand and silt) illustrated the same FT-IR spectra before (Spectra D and F) and after sorption (Spectra E and G), respectively, suggesting that there is not any sorption phenomenon, but only random positioning of the dye molecule on the surface of the material. In general, the anionic dye molecule may bind to the unspecific anion exchange sites in soil. Such sites are situated on the (hydr)oxides of iron and aluminum as well as at the edges of clay minerals (aluminol and silanol groups). As the pH of many soils is below their point of zero charge, iron and aluminum (hydr)oxides may serve as appropriate sorbents for anionic dyestuffs [44].

3.5. Economic aspect

Capital cost of installing PRBs is a concern especially with the cost of zero-valent iron, which is usually utilized as the proper medium. Iron nanoparticles a great extension of conventional zero-valent iron technology is moving rapidly to challenge clean-up problems. The price of nanoscale zero-valent iron has decreased in the past due to a decrease in the price of raw materials. Prices for 1000-pound quantities or more vary from US\$ 22–77/pound, depending on the quantity and quality [45]. On the other hand, bulk prices for chitosan vary significantly. The demand for chitosan has grown remarkably and production sites have been established in many countries worldwide. About 1–4 million pounds of chitosan could be produced at a cost of US\$ 1.00–2.00/pound [46]. Another conservative estimation, of the Planning Department of Uttar Pradesh, India, for chitosan is US\$ 4.5–5.2/pound [47]. Given that the process of making chitosan beads is not expensive, one could assume that the cost of chitosan is affordable. However, its potential applicability as treatment wall should be previously tested in large scale implementations.

4. Conclusions

In the present investigation, chitosan beads were prepared and evaluated as reactive barriers in the transport of the azo dye RB5 in a soil column. Chitosan beads presented (i) high sorption capacity ($S_{\text{max}} = 238\text{ mg/g}$), (ii) high pseudo-first sorption rates ($k_1 = 1.02\text{ h}^{-1}$) and (iii) increase in the retardation factor of soil roughly 80 times. Taking into account the previous characteristics of chitosan beads along with their low swelling ($\sim 35\%$), irreversibility and permeability over long time, it seems possible that they could be used as physical PRBs. A challenge would be the possibility of extending their application into chemical and biochemical transformations.

References

- [1] C. O'Neill, F.R. Hawkes, D.L. Hawkes, N.D. Lourenço, H.M. Pinheiro, W. Delée, Colour in textile effluents—sources, measurement, discharge consents and simulation: a review, *J. Chem. Technol. Biotechnol.* 74 (1999) 1009–1018.
- [2] T. Robinson, G. McMullan, R. Marchant, P. Nigam, Remediation of dyes in textile effluent: a critical review on current treatment technologies with a proposed alternative, *Bioresour. Technol.* 77 (2001) 247–255.
- [3] G.L. Baughman, Fate of dyes in aquatic systems. Part 3: The role of suspended sediments in adsorption and reaction of acid and direct dyes, *Dyes Pigments* 27 (1995) 197–210.
- [4] S.R. Blackburn, Natural polysaccharides and their interactions with dye molecules: applications in effluent treatment, *Environ. Sci. Technol.* 38 (2004) 4905–4909.
- [5] G. McKay, J.F. Porter, G.R. Prasad, The removal of dye colours from aqueous solutions by adsorption on low-cost materials, *Water, Air, Soil Pollut.* 114 (1999) 423–438.
- [6] G. Crini, Non-conventional low-cost adsorbents for dye removal: a review, *Bioresour. Technol.* 97 (2006) 1061–1085.
- [7] J. Germán-Heins, M. Flury, Sorption of brilliant blue FCF in soils as affected by pH and ionic strength, *Geoderma* 97 (2000) 87–101.
- [8] M.M. Scherer, S. Richter, R.L. Valentine, P.J.J. Alvarez, Chemistry and microbiology of permeable reactive barriers for *in situ* groundwater clean up, *Crit. Rev. Microbiol.* 26 (2000) 221–264.
- [9] K. Komnitsas, G. Bartzas, I. Paspaliaris, Inorganic contaminant fate assessment of zero-valent iron walls, *Environ. Forensics* 7 (2006) 207–217.
- [10] T.F. Guerin, S. Horner, T. McGovern, B. Davey, An application of permeable reactive barrier technology to petroleum hydrocarbon contaminated groundwater, *Water Res.* 36 (2002) 15–24.
- [11] M. Rinaudo, Chitin and chitosan: properties and applications, *Prog. Polym. Sci.* 31 (2006) 603–632.
- [12] A.R. Cestari, E.F.S. Vieira, J.A. Mota, The removal of an anionic red dye from aqueous solutions using chitosan beads—the role of experimental factors on adsorption using a full factorial design, *J. Hazard. Mater.* 160 (2008) 337–343.
- [13] G.Z. Kyzas, N.K. Lazaridis, Reactive and basic dyes removal by sorption onto chitosan derivatives, *J. Colloid Interface Sci.* 331 (2009) 32–39.
- [14] British Standards 1377-1, Methods of Test for Soils for Civil Engineering Purposes-Part 1: General Requirements and Sample Preparation, 1990.
- [15] H. Sontheimer, J.C. Crittenden, R.D. Summers, Carbon for Water Treatment, DVGW-Forschungsstelle, Karlsruhe, 1988.
- [16] OECD Guideline for Testing of Chemicals 106, Adsorption–Desorption. Using a Batch Equilibrium Method, 2000, Adopted by the council on 21 January 2000.
- [17] J.T. Angley, M.L. Brusseau, W.L. Miller, J.J. Delfino, Nonequilibrium sorption and aerobic biodegradation of dissolved alkylbenzenes during transport in aquifer material: column experiments and evaluation of a coupled-process model, *Environ. Sci. Technol.* 26 (1992) 1404–1410.
- [18] D.G. Kinniburgh, General purpose adsorption isotherms, *Environ. Sci. Technol.* 20 (1986) 895–904.
- [19] G. Gibbs, J.M. Tobin, E. Guibal, Influence of chitosan preprotonation on Reactive Black 5 sorption isotherms and kinetics, *Ind. Eng. Chem. Res.* 43 (2004) 1–11.
- [20] K.Z. Elwakeel, Removal of Reactive Black 5 from aqueous solutions using magnetic chitosan resins, *J. Hazard. Mater.* (2009), doi:10.1016/j.jhazmat.2009.01.051.
- [21] W. Tanthapanichakoon, P. Ariyadejwanich, P. Japthong, K. Nakagawa, S.R. Mukai, H. Tamon, Adsorption–desorption characteristics of phenol and reactive dyes from aqueous solution on mesoporous activated carbon prepared from waste tires, *Water Res.* 39 (2005) 1347–1353.
- [22] K. Vijayaraghavan, Y.-S. Yun, Utilization of fermentation waste (*Corynebacterium glutamicum*) for biosorption of Reactive Black 5 from aqueous solution, *J. Hazard. Mater.* 141 (2007) 45–52.
- [23] Y. Qiu, F. Ling, Role of surface functionality in the adsorption of anionic dyes on modified polymeric sorbents, *Chemosphere* 64 (2006) 963–971.
- [24] H.-D. Choi, M.-C. Shin, D.-H. Kim, C.-S. Jeon, K. Baek, Removal characteristics of reactive black 5 using surfactant-modified activated carbon, *Desalination* 223 (2008) 290–298.
- [25] O. Gulnaz, A. Kaya, S. Dincer, The reuse of dried activated sludge for adsorption of reactive dye, *J. Hazard. Mater.* 134 (2006) 190–196.
- [26] Y. Xue, H. Hou, S. Zhu, Adsorption removal of reactive dyes from aqueous solution by modified basic oxygen furnace slag: isotherm and kinetic study, *Chem. Eng. J.* 147 (2009) 272–279.
- [27] R. Patel, S. Suresh, Kinetic and equilibrium studies on the biosorption of reactive black 5 dye by *Aspergillus foetidus*, *Bioresour. Technol.* 99 (2008) 51–58.
- [28] Z. Eren, F.N. Acar, Adsorption of Reactive Black 5 from an aqueous solution: equilibrium and kinetic studies, *Desalination* 194 (2006) 1–10.
- [29] B.C. Oei, S. Ibrahim, S. Wang, H.M. Ang, Surfactant modified barley straw for removal of acid and reactive dyes from aqueous solution, *Bioresour. Technol.* 100 (2009) 4292–4295.
- [30] P. Pengthamkeerati, T. Satapanajaru, O. Singchan, Sorption of reactive dye from aqueous solution on biomass fly ash, *J. Hazard. Mater.* 153 (2008) 1149–1156.
- [31] J.F. Osma, V. Saravia, J.L. Toca-Herrera, S.R. Couto, Sunflower seed shells: a novel and effective low-cost adsorbent for the removal of the diazo dye Reactive Black 5 from aqueous solutions, *J. Hazard. Mater.* 147 (2007) 900–905.
- [32] M.S. Chiou, H.Y. Li, Adsorption behavior of reactive dye in aqueous solution on chemical cross-linked chitosan beads, *Chemosphere* 50 (2003) 1095–1105.
- [33] Y.S. Ho, J.C.Y. Ng, G. McKay, Kinetics of pollutants sorption by biosorbents: review, *Sep. Purif. Methods* 29 (2000) 189–232.

- [34] C.W. Cheung, J.F. Porter, G. McKay, Sorption kinetic analysis for the removal of cadmium ions from effluents using bone char, *Water Res.* 35 (2001) 605–612.
- [35] D.W. Marquardt, An algorithm for least-squares estimation of nonlinear parameters, *J. Soc. Ind. Appl. Mater.* 11 (1963) 431–441.
- [36] J. Šimůnek, M. Šejna, H. Saito, M. Sakai, M.Th. van Genuchten, The HYDRUS-1D Software Package for Simulating the One-Dimensional Movement of Water, Heat and Multiple Solutes in Variably-Saturated Media, US Salinity Laboratory, USDA-ARS, Riverside, CA, 2008.
- [37] Z. Li, H. Hong, Retardation of chromate through packed columns of surfactant-modified zeolite, *J. Hazard. Mater.* 162 (2009) 1487–1493.
- [38] A. Wehrhan, R. Kasteel, J. Šimůnek, J. Groeneweg, H. Vereecken, Transport of sulfadiazine in soil columns—experiments and modelling approaches, *J. Contam. Hydrol.* 89 (2007) 107–135.
- [39] A.J. Valocchi, Validity of the local equilibrium assumptions for modeling sorbing solute transport through homogeneous soils, *Water Resour. Res.* 21 (1985) 808–820.
- [40] R. Wibulswas, Batch and fixed bed sorption of methylene blue on precursor and QACs modified montmorillonite, *Sep. Purif. Technol.* 39 (2004) 3–12.
- [41] C.L. de Vasconcelos, P.M. Bezerril, D.E.S. dos Santos, T.N.C. Dantas, M.R. Pereira, J.L.C. Fonseca, Effect of molecular weight and ionic strength on the formation of polyelectrolyte complexes based on poly(methacrylic acid) and chitosan, *Biomacromolecules* 7 (2006) 1245–1252.
- [42] K. Takayama, M. Hirata, Y. Machida, T. Masada, T. Sannan, T. Nagai, Effect of interpolymer complex formation on bioadhesive property and drug release phenomenon of compressed tablet consisting of chitosan and sodium hyaluronate, *Chem. Pharm. Bull.* 38 (1990) 1993–1997.
- [43] A. Singh, S.S. Narvi, P.K. Dutta, N.D. Pandey, External stimuli response on a novel chitosan hydrogel crosslinked with formaldehyde, *Bull. Mater. Sci.* 29 (2006) 233–238.
- [44] H. Ketelsen, S. Meyer-Windel, Adsorption of brilliant blue FCF by soils, *Geo-derma* 90 (1999) 131–145.
- [45] A. Gavaskar, L. Tatar, W. Condit, Cost and Performance Report Nanoscale Zero-Valent Technologies for Source Remediation, Naval Facilities Engineering Command, Contract Report CR-05-007-ENV, September 2005.
- [46] V.K. Gupta, I. Ali, Adsorbents for water treatment: development of low-cost alternatives to carbon, in: Q. Somasundaran (Ed.), *Encyclopedia of Surface and Colloid Science*, 2nd ed., Taylor & Francis, New York, 2006, pp. 149–184.
- [47] <http://planning.up.nic.in/innovations/inno3/fi/Chitosan.htm>.